ACS OMEGA

http://pubs.acs.org/journal/acsodf

Article

Honokiol-Chlorambucil Co-Prodrugs Selectively Enhance the Killing Effect through STAT3 Binding on Lymphocytic Leukemia Cells *In Vitro* and *In Vivo*

Li Xia, Dali Kang, Dan Wan, Chu Chu, Meizi Chen, Shuihan Zhang, Xiong Li, Leye He, Jianye Yan, Teng Liu,* and Yongbo Peng*

Cite This: *ACS Omega* 2020, 5, 19844−19852

Read Online

ACCESS | Metrics & More | Article Recommendations | Supporting Information

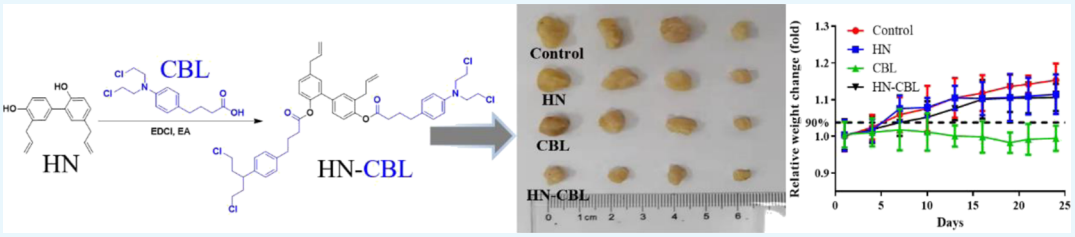

ABSTRACT: The broad-spectrum DNA alkylating therapeutic, chlorambucil (CBL), has limited safety and shows lower therapy effect because of a short half-life while used in the clinic. Therefore, it is very necessary to develop a more efficient and safer type of CBL derivate against tumors with selective targeting of cancer cells. In addition, the natural product of honokiol (HN), the novel potent chemo-preventive or therapeutic entity/carrier, can target the mitochondria of cancer cells through STAT3 to prevent cancer from spreading and metastasizing. In this study, we designed and synthesized the honokiol−chlorambucil (HN−CBL) co-prodrugs through carbonate ester linkage conjugating with the targeted delivery help of the HN skeleton in cancer cells. Biological evaluation indicated that HN−CBL can remarkably enhance the antiproliferation of human leukemic cell lines CCRF-CEM, Jurkat, U937, MV4-11, and K562. Furthermore, HN−CBL can also selectively inhibit the lymphocytic leukemia (LL) cell survival compared to those mononuclear cells derived from healthy donors (PBMCs), enhance mitochondrial activity in leukemia cells, and induce LL cell apoptosis. Molecular docking and western blot study showed that HN−CBL can also bind with the STAT3 protein at some hydrophobic residues and downregulate the phosphorylation level of STAT3-like HN. Significantly, HN−CBL could dramatically delay leukemia growth *in vivo* with no observable physiological toxicity. Thus, HN−CBL may provide a novel and effective targeting therapeutic against LL with fewer side effects.

1. INTRODUCTION

Chlorambucil (CBL), a DNA alkylating reagent belonging to the nitrogen mustard family, is a chemotherapeutic used to treat chronic lymphocytic leukemia (CLL), lymphoma, and many other types of solid neoplasms.[1,2] The *N*,*N*-bis(2-chloroethyl)-amine group moiety can covalently react with proteins, nucleic acids, and phospholipids to induce inhibitory function for cell survival, while the CBL alkylation reaction with DNA is the primary form of cytotoxicity. In addition, the forms of CBL-modifying DNA cross-link include monofunctional base-pair mismatching and bifunctional double-strand DNA breaking, which cause sustained DNA damage.[3,4] Because of the high reactivity of CBL with lots of biological macromolecules (nucleic acids, proteins, and phospholipids), which leads to the lower therapeutic effect with a short half-life in clinic and means a higher dose of CBL is required for the therapeutic response. However, an increased dose will increase the risk of severe side effects. In addition, these compounded consequences of instability and nonspecificity reactivity will bring down the bioaction rate of CBL. For now, although some newer drugs have been successfully developed for clinical application, the fact is that CBL remains a first-line treatment for the elderly CLL and some immune-suppressed cancer persons. Therefore, it is very important to develop the novel CBL derivatives with a higher anticancer effect and stable hypotoxicity for normal healthy tissues.[5−7]

Honokiol (HN, $C_{18}H_{18}O_2$) is an isolated dietary biphenolic natural product from *Magnolia officinalis*. During the last decade, lots of studies have shown that HN exhibits a broad inhibitory effect on malignant carcinomas (e.g., myeloma and leukemia[8,9]) *in vitro* and *in vivo* through anticarcinogenic, proapoptotic, anti-

Received: June 14, 2020
Accepted: July 17, 2020
Published: July 29, 2020

Scheme 1. Synthesis Route of HN−CBL Co-Prodrugs

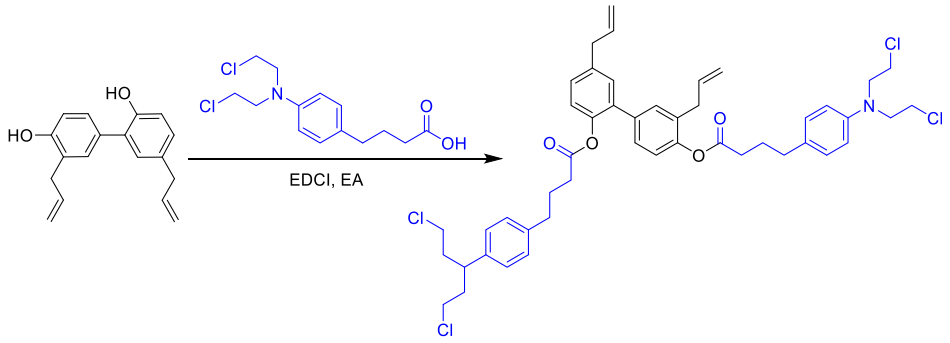

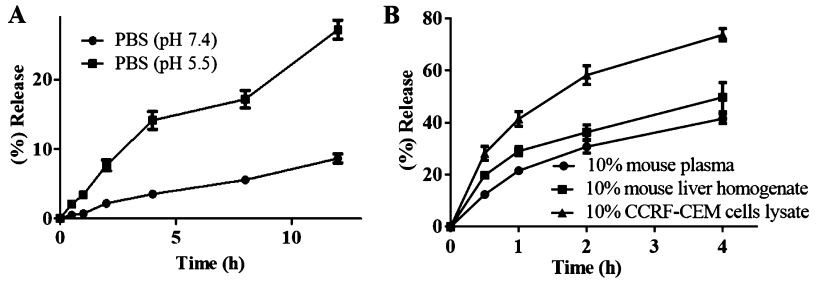

Figure 1. Targeted release pharmacokinetics of HN−CBL in the cancer microenvironment. (A) Degradation of the co-prodrugs HN−CBL in PBS (pH = 7.4) and PBS (pH = 5.5); (B) HN−CBL responsively released from the co-prodrugs in bio-mediums (10% mouse plasma, 10% mouse liver homogenate and 10% CCRF-CEM cells lysate at 37 °C).

inflammatory, antioxidative, and antiangiogenic activities without any observable sub-toxicities. Furthermore, HN can effectively inhibit many pathways and lead to anti-proliferation of cancer cells, such as the cell signaling of NF-kB, EGFR, STAT3, cyclooxygenase, and the other cell apoptosis factor, and so forth. Meanwhile, HN can also overcome even notoriously drug-resistant neoplasms.[10] In addition, HN was considered to be nearly as effective as an antitumoral drug against colorectal cells and equal to the common chemotherapeutic adriamycin (DOX). Very importantly, HN can target cancer cells' mitochondria through STAT3 to halt cancer progression and metastasis, which indicated that HN could be the novel potent chemo-preventive or therapeutic entity for tumor treatment.[11,12] Although clinical studies are still lacking, HN possesses so many beneficial bio-effects against cancer with high safety characteristics, which suggests that HN is a promising potential antitumor agent and carrier for targeting cancer treatment, especially the hydroxyl group of HN is an excellent ligand for drug carriers.[12]

Based on the above molecular mechanism backgrounds of CBL and HN, we think that the development of the novel antitumor reagents from the approved therapeutics or the safe dietary natural products, rather than any other unknown compounds, would promote their transformation and application in cancer therapy. To complete the above proof-of-concept of enhancing the killing effect on cancer cells through co-prodrugs, and based on the biologic basis of higher esterase and low pH in the tumor tissue or cancer cells,[13,14] we designed and synthesized a honokiol−chlorambucil (HN−CBL) ester co-prodrugs through carbonate ester linkage conjugation (Figure S1). In our report, the releasing response mechanism of HN−CBL was that the double carbonic ester conjugated with HN and CBL, which can be simply hydrolyzed in higher intracellular esterase's hydrolysis catalyzed environment (e.g., the cancer cells lysates) and is especially sensible to the tumor acid microenvironment (as pH = 5.5 vs pH = 7.4). When evaluating the inhibitory effect on a series of carcinoma and normal cell lines with *in vitro* MTT cytotoxicity methods, HN−CBL, exhibited better therapeutic potency than its parent drugs HN and CBL through directly enhancing mitochondrial activity. HN−CBL could selectively enhance the killing effect in lymphocytic leukemia (LL) cells, and no red blood cells hemolysis reaction was observed at the therapeutic concentration of HN−CBL. Moreover, HN−CBL could remarkedly enhance the apoptosis in LL cells but had no damage on normal PBMCs. The computational docking and western blotting study showed that HN−CBL can also bind with the STAT3 protein at some hydrophobic residues and downregulate the phosphorylation level of STAT3-like HN. Above all, HN−CBL could dramatically delay leukemia growth *in vivo* with no observable physiological toxicity. Compared with free drugs, these results indicated that HN−CBL may provide a novel and selectively therapeutic co-prodrugs against LL with fewer side effects.

2. RESULTS AND DISCUSSION

2.1. Chemical Preparation and Characterization of the HN−CBL. The synthetic route of HN−CBL (Figure S1) is depicted in Scheme 1. HN−CBL was prepared from CBL which underwent an esterification reaction giving the carboxy group-containing HN, in the presence of EDCI. The purity of HN−CBL was >95% and measured with HPLC (Figure S2). The synthesized target compound HN−CBL was confirmed by ^{1}H NMR (Figure S3), mass spectrometry, and UV−vis spectrophotometer (Figure S4).

2.2. *In Vitro*-Targeted Release Pharmacokinetics of HN−CBL in Cancer Cells. Based on the cleavage lysis feature of co-prodrugs HN−CBL with carbonate ester by intracellular esterase's hydrolysis catalyzed and then released the drugs CBL and HN in biological mediums, such as PBS and plasma, especially in the tumor tissue or cancer cells with higher content of esterase and low pH.[14] To prove the above intuitive

https://dx.doi.org/10.1021/acsomega.0c02832
ACS Omega 2020, 5, 19844−19852

Table 1. IC_{50} Values (μM) of HN, CBL, HN−CBL, and HN−CBL in Different Cell Lines (72 h)[a]

cell line	CBL	HN	HN−CBL	HN−CBL	fold index for CBL
CCRF-CEM	6.73 ± 0.55	13.97 ± 0.59	5.89 ± 0.51	1.09 ± 0.27	~6.6
Jurkat	6.75 ± 0.71	10.60 ± 0.89	6.63 ± 0.65	1.15 ± 0.37	~6.4
U937	8.87 ± 0.77	11.90 ± 1.46	8.51 ± 0.62	1.29 ± 0.54	~6.8
MV4-11	17.90 ± 1.03	18.50 ± 2.33	17.06 ± 1.47	2.78 ± 0.46	~6.4
K562	25.90 ± 3.95	23.70 ± 2.66	21.89 ± 3.12	4.86 ± 0.71	~5.3
A549	>80	>80	>80	25.10 ± 4.77	>3.0
HepG2	>80	51.70 ± 6.68	48.81 ± 5.79	24.50 ± 3.91	>3.0
LO2	>80	>80	>80	>160	>0.5
NIH3T3	>80	>80	>80	>160	>0.5

[a]The mixture of HN and two equivalents CBL was named HN−CBL, and the cell cytotoxicity was detected with a MTT colorimetric assay, and each treated in triplicate.

hypothesis of co-prodrug, HN−CBL, HPLC−MS method was used to evaluate the drug release of HN or CBL in different mediums. The hydrolysis release of HN or CBL from co-prodrug HN−CBL was measured at 37 °C in different bio-mediums (as PBS in pH = 7.4 or 5.5, 10% fresh plasma and 10% cancer cells lysate.). The degradation of HN−CBL and the production of HN or CBL were measured with HPLC−MS technology. From the results of Figure 1, we found that only <10% of HN−CBL was hydrolyzed in normal isosmotic buffer PBS of pH = 7.4, but it would release more than 25% of free drugs in PBS of pH = 5.5, which proved that the co-prodrug HN−CBL has the tumor acid microenvironment sensibility response characterization. Meanwhile, when HN−CBL was incubated with 10% fresh mouse plasma including PBS (pH = 7.4), there was about 40% HN or CBL released from HN−CBL, but which would release more than 70% products in 10% CCRF-CEM cancer cell lysate with pH = 7.4 at 37 °C. The hydrolysis difference might attribute to the higher esterase expression in cancer cells.[15] In addition, the 10% normal mouse liver tissue was used to verify the above hypothesis, and we found that HN−CBL could keep much more bio-stable than that of the CCRF-CEM cells lysate (about 50% vs 70%). Therefore, these results indicated that the HN−CBL co-prodrugs can release free drugs HN and CBL well for synergistic effects, which will improve the specificity of CBL toward cancer cells, thus decrease the risk of side effects.

2.3. HN−CBL Selectively Inhibited Leukemia Cell Proliferation. In this study, the anticancer effects of co-prodrugs HN−CBL on a total of seven cancer cell lines were investigated by the MTT assay. Our data showed that the treatment of compound HN−CBL efficiently decreased the survival of seven tested carcinoma cell lines, as lymphocytic carcinoma CCRF-CEM (IC_{50} = 1.09 μM), Jurkat (IC_{50} = 1.15 μM), U937 (IC_{50} = 1.29 μM), MV4-11 (IC_{50} = 2.78 μM), K562 (IC_{50} = 4.86 μM), lung cancer A549 (IC_{50} = 25.10 μM), and human hepatoma HepG2 (IC_{50} = 24.50 μM) cells, and no observable cytotoxicity on two normal cells LO2 and NIH3T3. These results suggested that HN−CBL has a relatively wide antitumor spectrum, especially in leukemia cells with selectivity. In addition, the IC_{50} values of HN−CBL were lower than that of CBL and HN in the seven human cancer cell lines tested, which indicated that HN−CBL's synergistic antitumor activity was more potent than that of both HN and CBL (Table 1).

2.4. HN−CBL Selectively Inhibited Human Primary LL Cell Survival. In particular, it was notable that compound HN−CBL effectively reduced the cell survival of the carcinoma cells CCRF-CEM, U937, MV4-11, Jurkat, and K562 (IC_{50} = 1.09−4.86 μM). Because the co-prodrug HN−CBL decreased the survival of leukemia cells more efficiently, we continue to investigate the antiproliferation profile of co-prodrug HN−CBL and the therapeutic window in primary LL cells (Figure 2). To

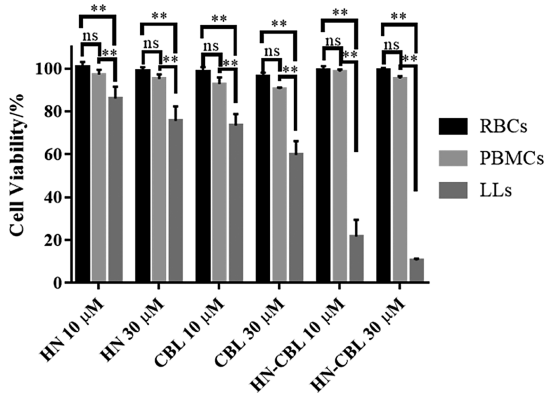

Figure 2. Bioactivity and therapeutic window of HN−CBL in donors' cells. HN, CBL, and HN−CBL activity in healthy donors' RBCs, mononuclear cells (PBMCs), and peripheral blood lymphocytes of patients with LLs. Percent cell viability was determined by MTT staining. The index values = mean values ±SEM, $n > 3$. And ns for no significant difference, * for p value < 0.05 and ** for p value < 0.01.

compare the toxicity of HN−CBL on the healthy cells, MTT colorimetric method was performed on three types of donor cells including the healthy RBCs, the healthy PBMCs, and the B cells isolated from LL patients. Compared with free drugs HN or CBL, HN−CBL did not produce RBC-hemolysis reaction at the tested concentrations (Figure S5), which implicated that HN−CBL can ablate the leukemia cells with low side effects. Compared to those derived from healthy donors, HN−CBL more preferred to target and kill the leukemia cells of LL patients than CBL, which was consistent with the release pharmacokinetic results of HN−CBL showing HN−CBL's cancer cell specificity because of the relative higher esterase activity and lower pH value in cancer cells.

2.5. HN−CBL-Enhanced Mitochondrial Activity in Leukemia Cells. It is well known that anticancer drug CBL has a high alkylating function, and its antileukemia bioactivity is focused on the cellular nuclear genome of cancer cells.[16] In this study, the natural product HN was used to co-deliver the CBL, which can target cancer cells' mitochondria (mt) through STAT3 to halt cancer progression and metastasis.[12] In addition, mt-DNA damage will increase ROS levels and change mt's membrane potential.[17,18] Therefore, to confirm the relation of HN−CBL-inducing cell death and the mitochondria, two mt'

https://dx.doi.org/10.1021/acsomega.0c02832
ACS Omega 2020, 5, 19844−19852

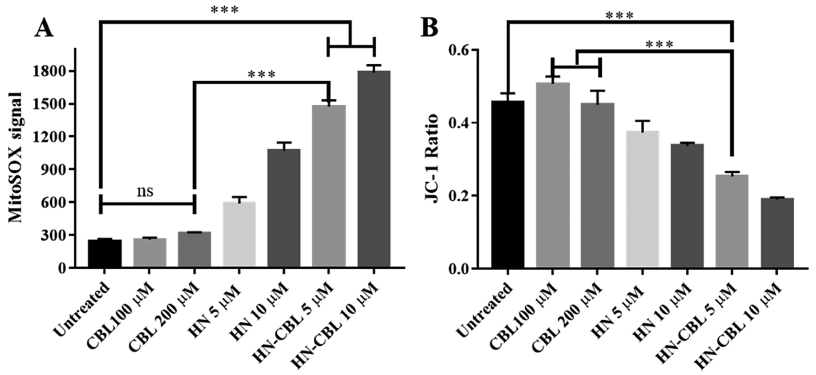

Figure 3. HN−CBL increased superoxide and depolarized mitochondrial membrane potential in Jurkat cells. (A) Increased levels of superoxide with the mitochondrial targeting of HN−CBL in Jurkat cells. (B) HN−CBL reduces the mt-membrane potentials in Jurkat cells. The index values = mean values ± SEM, $n = 3$. *t*-Test was used to calculate *p* values. Moreover, ns for no significant difference, ** for *p* value < 0.01 and *** for *p* value < 0.005.

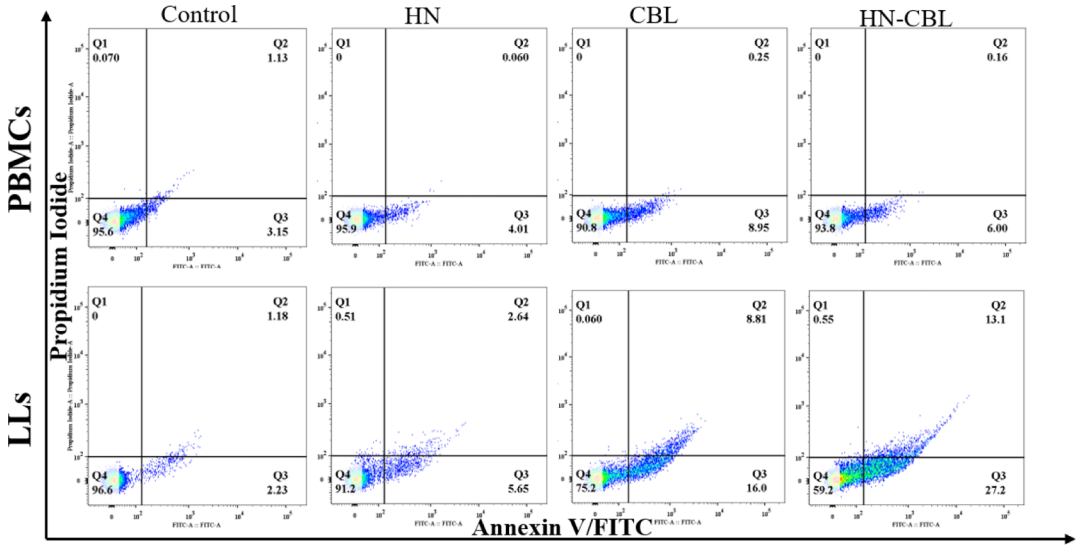

Figure 4. Flow cytometry analysis of HN−CBL in LL and healthy donors' mononuclear cells (PBMCs). HN−CBL can selectively increase in the apoptotic cell population in LL cells, but not observably damage on the normal PBMCs.

bio-marks, ROS levels and mt' membrane potential were detected with flow cytometry. While the leukemia cells were treated with HN−CBL, we observed that the superoxide concentration was increased and the mt' membrane potential was reduced (Figure 3A,B). However, the nuclear genome cross-linking agent CBL did not statistically change mt' superoxide levels and its membrane potential. These data supported the concept that HN−CBL is selectively destructive on the mitochondrial organelle.

2.6. HN−CBL-Induced LL Cell Apoptosis but No Damage on Normal PBMCs. Apoptosis is a programmed way that can induce cell death, and it has been proved that the mitochondria are involved in apoptosis through different mechanisms.[19] Moreover, our results showed that HN−CBL can induce cancer cell death through the activity on mitochondria. Thus, the cell apoptosis experiments of Annexin V-FITC/PI staining were used to determine the inhibitory effects of HN−CBL on leukemia cells. PBMCs and LL cells were incubated with HN, CBL, and HN−CBL for 24 h. The obtained apoptosis analysis showed that HN did not indicate an statistical difference in the apoptotic percentage in LL cells as well as untreated cells (about 7.5 vs 4.8%), and CBL could remarkedly induce CLL cell apoptosis by about 25%, and the significant LL cell death response was observed between HN−CBL treatment and CBL (about 40 vs 25%). However, no damage was observed on PBMCs (Figure S6). These results indicated that the cell apoptosis signal may be the main mechanism that co-prodrug HN−CBL exerts the higher bioactivity on leukemia cells than on CBL and HN (Figure 4). Our results indicated that the conjugation of HN and CBL can improve the anticancer activity of CBL and HN, and HN−CBL may be a novel chemotherapeutic for further investigation.

2.7. Molecular Docking for HN and HN−CBL Interaction with STAT3. In previous reports, HN was proved to target cancer cells' mitochondria (mt) through STAT3 to halt cancer progression and metastasis.[12] To explore the possible targeted delivery mechanism for HN−CBL, we further determined the interaction of HN or HN−CBL and STAT3 in silico. Molecular docking experiments were conducted for HN or HN−CBL and the crystal structure of STAT3 (PDB code: 3CWG) by Sybyl-X 2.1.1 software following the rule of the lower the energy was, the better the docking orientation. HN bound to STAT3 through alkyl and pi−alkyl interaction with a cluster of hydrophobic residues from each domain: ILE-467, HIS-332, PRO-471, and MET-470 (Figure 5A,B), which agreed with the reported STAT3 inhibitor CuB.[20] In addition, the hydrogen or oxygen atom of HN can form a hydrogen bond with the oxygen or hydrogen atom on the amino acid of LYS-573,

https://dx.doi.org/10.1021/acsomega.0c02832
ACS Omega 2020, 5, 19844−19852

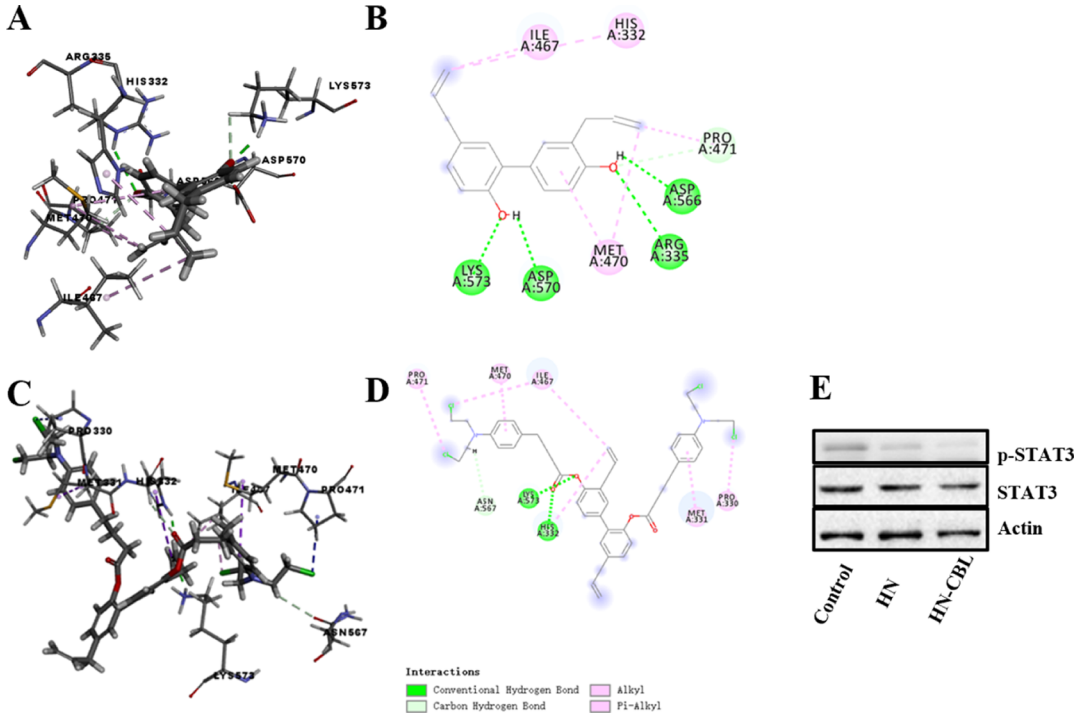

Figure 5. Molecular docking analysis for HN or HN−CBL with STAT3 and western blotting study. (A,C) Molecular binding mode of HN and HN−CBL docked into the target STAT3. (B,D) Details of binding sites of the HN and HN−CBL in STAT3 protein. (E) While leukemia cells were treated with HN or HN−CBL (10 μM) for 12 h, and the collected cell lysates were subjected to western blotting analysis.

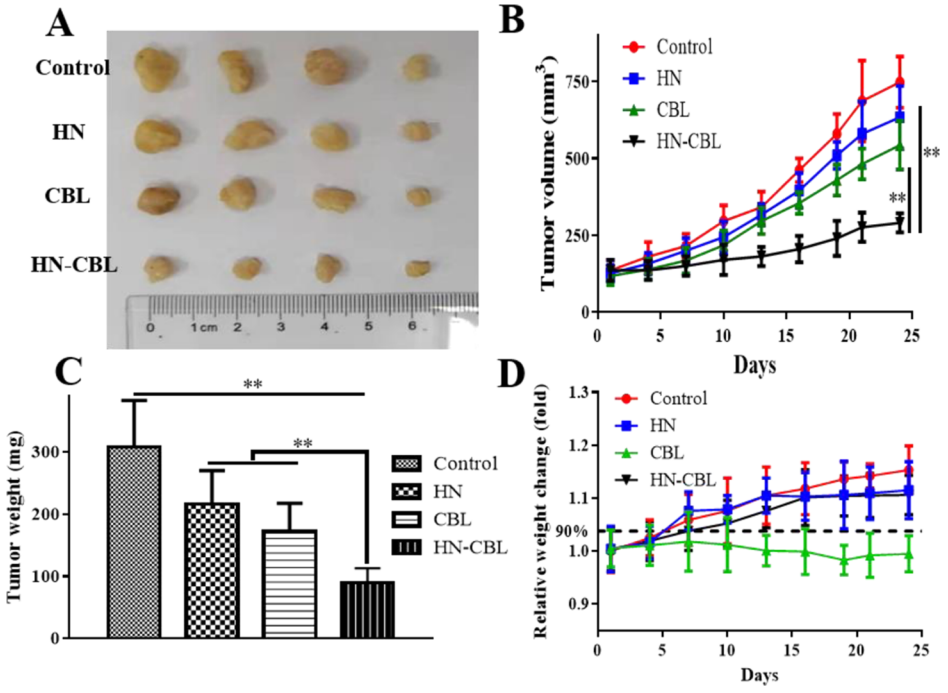

Figure 6. *In vivo* xenograft anti-LL study. (A) Photo images of the harvested tumors with different treatment. (B) Antitumor volume change difference, the sacrificed tumor weight index (C) and its relative weight changes (D) between control and the other drug treatments. Note that *, $p < 0.05$; **, $p < 0.01$, compared with the solvent control group.

ASP570, ARG-335, and ASP-566 in STAT3. The formation of the hydrogen bond enhances HN to target the STAT3 protein. Very interesting, the co-prodrug HN−CBL was also bound to STAT3 as HN through alkyl and pi−alkyl interaction with a cluster of hydrophobic residues from each domain: ILE-467, HIS-332, PRO-471, MET-470, PRO-330, and MET-331 (Figure 5C,D), which indicated that HN−CBL maintains maximally the binding activity with STAT3. In addition, the hydrogen or oxygen atom of HN−CBL can form a hydrogen bond with the oxygen or hydrogen atom on the amino acid of LYS-573 and HIS-332, the hydrogen atom of HN−CBL can form a carbon hydrogen bond with the carbon atom on the

https://dx.doi.org/10.1021/acsomega.0c02832
ACS Omega 2020, 5, 19844−19852

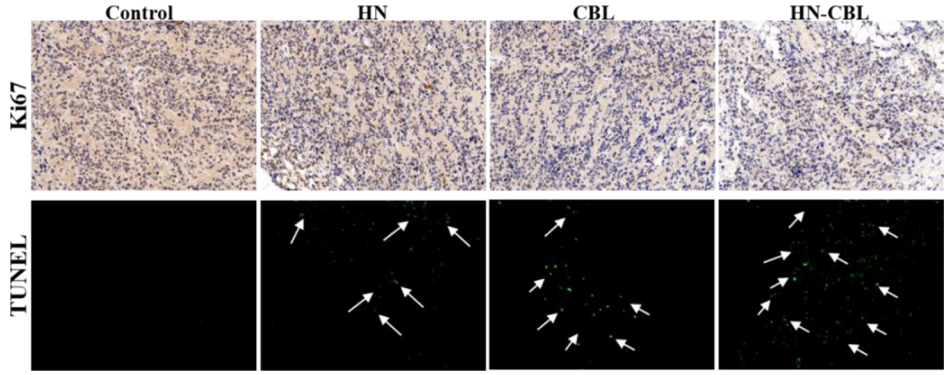

Figure 7. Ki-67 and TUNEL immunohistochemical staining of the harvested tumors treated with solvent control, HN, CBL, and HN−CBL co-prodrugs, respectively. In addition, the brown nucleus shows that the proliferation cells in Ki67 staining tumor tissues, the white row indicated the apoptosis tumor cells in TUNEL fluorescence analysis.

amino acid of ASN-567. The molecular docking analysis indicated that HN−CBL can bind the STAT3 protein as HN. In addition, the western blotting showed that HN−CBL can markedly inhibit the phosphorylation expression of STAT3(p-STAT3) with HN.[12] These results proved that HN−CBL produced its targeted killing effect in leukemia partially through the STAT3 interaction as HN.

2.8. HN−CBL Anti-LL Effects *In Vivo*. To further demonstrate the *in vivo* anti-CLL efficacy of HN−CBL, the BALB/c murine CEM xenograft model was used in this section. Equimolar dosage of HN (3.5 mg/kg), CBL (8 mg/kg), HN−CBL (11 mg/kg), and solvent control was administrated via iv tail injection every two days, respectively. The subcutaneous tumor volumes (V) and nude mice weights (M) were traced for 24 days with a four-day interval. From the Figure 6, we can observe that both of HN, CBL, and HN−CBL could effectively reduce tumor growth than the control treatment, and the treatment of HN−CBL could significantly inhibit tumor volume for the HN or CBL group on the 13th day (Figure 6B). Also, the obtained tumor tissues are photographed and weighted in Figure 6A,C. Compared to HN or CBL, the photograph size and intrinsic tumor weight show that HN−CBL could enormously inhibit the leukemia cell proliferation by reducing cancer cell growth. While, Figure 6D shows that the CBL causes body weight loss, which reflect serious physio-toxicity in mice. Very interesting, the group of HN−CBL treatment can keep the mice weights stable during the time of therapy, which is like the solvent control and HN group. These interesting results suggesting that HN−CBL could lower the physio-toxicity caused by CBL in mice. Probably because of the high reactivity of CBL with lots of biological macromolecules, which leads to the lower therapeutic effect with a short half-life in clinic and means that a higher therapeutic dose of CBL will increase the risk of severe side effects.[3,4]

The major organs of varied treatments were harvested for pathological analysis via H&E staining (Figure 7) on the 24th day. Major organs of the HN−CBL group showed no observed tissue injury compared with the control group, while the CBL treatment induced liver damage (Figure S7). However, the proliferation and apoptosis of the tumor tissue was further determined by immunohistochemical of Ki-67 staining and TUNEL fluorescence. As shown in Figure 7, lower proliferative cell rates were found in both drug-treated groups compared with the solvent group. In addition, the Ki-67 positive cells of HN−CBL-treated groups were reduced more than HN or CBL increased. While more apoptotic cells were observed in HN−CBL-treated groups in TUNEL fluorescence (Figure 7). Considering the anti-leukemia efficacy (Figure 6) and related physio-damage of main organs (Figure S7), HN−CBL co-prodrugs may be a novel chemotherapeutic in leukemia therapy with excellent antitumor efficacy and lower side effects.

3. CONCLUSIONS

Because of the ester prodrug design has practical approaches to improve the drug bioavailability and efficiency through enhancing the bio-membrane permeability and reducing nonspecific toxicity. In our report, based on the targeted delivery help of the honokiol skeleton in cancer cells, the combination of the broad-spectrum DNA alkylating therapeutics chlorambucil and the safe dietary natural product honokiol, a novel conjugated co-prodrug of HN−CBL was designed and synthesized. Biological evaluation data showed that co-prodrug HN−CBL can observably inhibit the proliferation of many carcinoma lines, particularly the LL lines, compared to the healthy PBMCs' toxicity of HN−CBL, which can selectively kill LL cells of patients with LL. Moreover, HN−CBL can enhance mitochondrial activity in leukemia cells and induce leukemia cell apoptosis. In a proof of concept, molecular docking and western blot study showed that HN−CBL can also bind with the STAT3 protein at some hydrophobic residues and downregulate the phosphorylation level of STAT3-like HN. *In vivo* xenograft, HN−CLB could significantly reduce LL tumor growth. It is noteworthy that no significant physiological toxicity are observed in the HN−CBL group; however, the liver tissue injury was determined in the CBL-treated group. Together, these results showed that the co-prodrug HN−CBL could be a promising anti-LL agent with fewer side effects than CBL, while the mitochondrial dysfunction and cell apoptosis might be the main antiproliferation mechanisms.

4. MATERIALS AND METHODS

4.1. Reagents and Characterization. Chlorambucil (CBL, HPLC pure >95%), Honokiol (HN, HPLC pure >95%), *N*-ethyl-*N*′-(3-dimethylaminopropyl) carbodiimide hydrochloride (EDCI), *N*,*N*-dimethylformamide (DMF), dimethyl sulfoxide (DMSO), ethyl acetate, and sodium sulfate were purchased from Energy Chemical (Shanghai, China). Chromatographic purity acetonitrile (ACN) was from Thermo fisher. MTT (98%) was from MedChemExpress (Shanghai, China). A cell apoptosis assay kit of Annexin V-FITC and the other cell experimental regents were come from Life Gibco

https://dx.doi.org/10.1021/acsomega.0c02832
ACS Omega 2020, 5, 19844−19852

Technologies in Thermo Fisher (Grand Island, USA). The antibody of p-STAT3 (#9134S), STAT3 (9139S), and Actin were purchased from Cell Signaling Technology (Danvers, MA).

^{1}H NMR spectra were recorded on a Bruker AM-400 NMR spectrometer in deuterated chloroform ($CDCl_3$). The chemical shifts are reported in δ (ppm) relative to tetramethylsilane (TMS) as an internal reference. High-resolution mass spectra (HRMS) were recorded on an Agilent 1260 UPLC-Waters Q-TOF micro mass spectrometer. Agilent 1260 ultra-high-performance liquid chromatography with a C18 column and UV−vis detector were used to determine the HN−CBL release following the molecular ion mass charge ratio.

4.2. Chemical Synthesis and Identification for HN−CBL. About 180 mg of CBL (0.59 mmol), dissolved in 5 ml of DMF, was added with EDCI (∼135 mg, 0.70 mmol) and then the solution was stirred for 10 min at room temperature. Then, HN (75 mg, 0.28 mmol) was added and the reaction mixture was stirred overnight at room temperature. The reaction solution was added with 50 mL of ethyl acetate and then washed once with 50 mL of water, dried by sodium sulfate, filtered, and concentrated. The yellow solid was purified by chromatography with a yield of 10%. ^{1}H NMR(400 MHz, $CDCl_3$): δ 1.85−1.86 (m, 1H), 2.09−2.12 (m, 2H), 2.18−2.19 (m, 1H), 2.40−2.42 (m, 2H), 2.49−250 (m, 1H), 2.64−2.66 (m, 2H), 2.71−2.73 (m, 2H), 2.73−2.85 (m, 1H), 3.37−3.45 (m, 4H), 3.68−3.70 (m, 8H), 3.73−3.76 (m, 8H), 5.09−5.71 (m, 2H), 6.65−6.71 (m, 4H), 6.96−7.00 (m, 1H),7.02−7.08 (m, 2H), 7.12−7.22 (m, 7H),7.30−7.31 (m, 2H), 7.37−7.39 (m, 2H). MS (ESI): 839.7 ($C_{46}H_{52}Cl_4N_2O_4$) $[M + H]^+$, and the calcd value of m/z is 838.6.

4.3. UPLC−MS Analysis of HN−CBL Co-Prodrugs. While differently treated for HN−CBL, the injection sample volume was 10 μL, the column temperature compartment was at 25 °C. The mobile phase containing 0.1% formic acid (FA)/acetonitrile (ACN) and 0.1% FA/H_2O was used to separate HN, CBL, and HN−CBL with flow rate at 1 mL/min, and the gradient elution was at 0−10min(4% ACN to 96% ACN) and 10−15 min(96% ACN).

4.4. Cell Culture and Buffer Conditions. CCRF-CEM, Jurkat, U937, MV4-11, K562 and LO2 cells were purchased from ATCC (Bethesda, MD, USA) or from CTCC (CAS, Shanghai, China) and were cultured in DMEM or RPMI 1640 media (Gibco) supplemented with 10% (v/v) fetal bovine serum (FBS, Gibco) and 100 units of antibiotics (Gibco) in an incubator with a 5% CO_2 atmosphere and 37 °C environment. Fresh leukemia mononuclear cells (LLs) from the peripheral blood of LL patients (LLs classified into subtypes based on the French−American−British (FAB) classification system) and healthy peripheral blood monocyte (PBMCs) were purified by Ficoll buffer. Red blood cells (RBCs) were also obtained during Ficoll separation of peripheral blood from healthy donors. Informed consent was obtained according to institutional guidelines. Mononuclear cells were suspended in RPMI 1640 medium containing 20% FBS at a density of approximately 5−10 × 10^5/mL for treatment. Dulbecco's phosphate buffered saline without Ca^{2+} and Mg^{2+} (DPBS, Invitrogen) was used to wash cells.

4.5. Collection of Clinical Biospecimens and Hemolysis Determining. According to a protocol approved by a research ethics board, peripheral blood lymphocytes of healthy donors was purified and named PBMCs, and lymphocytes of LL patients was named LLs. Peripheral blood mononuclear cells were isolated by Ficoll centrifugation. Red blood cells (RBCs) were separated from healthy donors' blood and purified with cooled PBS. CBL, HN, and HN−CBL solutions were prepared in isotonic buffer, and then added to RBCs' buffer for hemolysis analysis in 96-well plate. Simply, each well, 2 μL of RBCs were added, mixed, and then incubated for 1 h at 37 °C with 5% CO_2. For 100% lysis, 50% H_20 was added to wells, and for negative control (0%), cells from those wells only including PBS buffer were used. When centrifugal for 10 min at 1000*g*, the supernatant was then transferred to those new tubes, PBS was added and mixed, and read at 450 nm to determine absorbances. The above cells were fresh.

4.6. Cytotoxicity Determination with MTT Method. Briefly, A549, HepG2, NIH3T3, and LO2 cells were seeded at a density of 4−6 × 10^3 cells/well in 96-wells plates. Leukemia cell lines (CCRF-CEM, Jurkat, U937, MV4-11 and K562) were seeded at a density of 10−20 × 10^3 cells/well in 96-well flat-bottom plates. In addition, the detailed experimental processes are described as the cited paper.[21] The IC_{50} values and statistical analysis were performed using GraphPad Prism 5.01 (GraphPad Software).

4.7. Determination of Superoxide in Mitochondria. Following the manual of the superoxide kit (Invitrogen), we have plated 4 × 10^4 leukemia cells in a 12-well panel for the treatment of CBL, HN, or HN−CBL. When the mixture of cells and drugs were incubated for 1.5 h, we first removed the media, and then completed the processes of trypsin digestion and centrifugation; the obtained cells were stained with MitoSOX and analyzed with a BD FACSVerse flow cytometer (BD Biosciences, Ann Arbor, MI).

4.8. Membrane Potentials of Mitochondria Analysis. To compare the mitochondrial membrane potential difference between untreated and treated with HN, CBL, or HN−CBL, the Beyotime' JC-1 kit was used to determine. In addition, the detailed experimental processes followed the protocol of the manufacturer and the cited paper.[21]

4.9. Apoptosis Analysis. Under the help of a BD FACSVerse flow cytometer (BD Biosciences, CA), the apoptosis in PBMC and LL cells was measured after treatment without or with HN, CBL, and HN−CBL for 24 h. When the target cells were harvested with PBS, following the manual of the apoptosis kit of Annexin V-FITC/PI from Beyotime (China), we compared the difference between untreated and treated with HN, CBL, or HN−CBL.

4.10. Molecular Docking Study of HN−CBL Co-Prodrugs and HN. Molecular ligand docking studies were performed with the Sybyl-X 2.1.1 software, whose energy minimized using the default parameters. The X-ray crystal structure of STAT3 (PDB code: 3CWG) was obtained from the protein data bank. The chemical structure of HN and HN−CBL is shown in Figure S1. Docking was performed with the docking box sizes large enough to include the binding sites.

4.11. Western Blotting. While the LL cells were treated with 10 μM HN or HN−CBL for 12 h, and the collected cells were lysed in 200 μL of WB&IP lysis buffer (1% Triton X-100), including 1 mM PMSF (Beyotime, China). Protein extracts (50 μg) were loaded onto an 8−15% polyacrylamide gel containing SDS, electrophoresed, and transferred to a 0.22 μm nitrocellulose membrane (PALL, USA). The membranes were blocked with 5% non-fat dried milk in Tris-buffered saline containing 0.1% Tween 20 (TBST) and incubated overnight at 4 °C with the primary antibody. The blots were washed with TBST three times and then probed with HRP-conjugated

https://dx.doi.org/10.1021/acsomega.0c02832
ACS Omega 2020, 5, 19844−19852

secondary antibodies for 2 h at room temperature. The immune complexes were visualized using a Phototope-HRP Western Blot Detection System (Pierce, USA) as previously reported.[22] Actin was used to ensure equivalent loading of the whole cell protein. All data were confirmed by three individual experiments.

4.12. *In Vivo* Xenograft Model. Female BALB/c-Nude mice (4−6 weeks old) were obtained from the Hunan Laboratory Animal Center (Changsha, China). All animal studies were performed according to protocols approved by the Institutional Animal Care and Use Committee (IACUC) of the Hunan Academy of Traditional Chinese Medicine. After acclimatized to their new environment for five days, the mice were injected subcutaneously with CCRF-CEM cells (1.2×10^7/0.2 ml/mouse) into the flank (day 0). When the tumor volume reached about 100 mm^3, the mice were divided randomly into four groups, and then given intravenously of solvent control, HN (3.5 mg/kg), CBL (8 mg/kg), and HN−CBL co-prodrugs (11 mg/kg, is equivalent to at the HN dosage of 3.5 or 8 mg/kg of CBL) every two days, respectively. The volumes of tumor (V) and mice weights were recorded every three days, calculated using the formula $V = (a \times b^2)/2$, where "a" and "b" represents the length and width of the tumor diameters, respectively. After the experiments were finished, mice were sacrificed on day 24 of treatment, the tumors and main organs were harvested and fixed in formaldehyde for the further paraffin embedding.

4.13. Detection of TUNEL Apoptosis and Ki67 Proliferation Analysis in Tumor and H&E Staining of Main Organ. The tumor tissues apoptosis was detected by a TUNEL detection kit (Roche). Simply, the tumor tissues of paraffin-embedded specimens were dewaxed in xylene and rehydrated with decreasing concentrations of ethanol.[22] In addition, the cell proliferation of tumor tissues was analyzed by a immunohistochemical staining assay of Ki-67 using the labeled streptavidin-biotin method. The morphology of main organs was evaluated by hematoxylin and eosin (H&E) staining.

4.14. Statistical Analysis. For analysis of data, values were presented as mean ± SEM for the independent experiments. Statistical differences were determined by nonpaired Student's two-tailed t-test and $p < 0.05$ was considered statistically significant.

■ ASSOCIATED CONTENT

Supporting Information

The Supporting Information is available free of charge at https://pubs.acs.org/doi/10.1021/acsomega.0c02832.

Chemical structure, HPLC profile, ^{1}H NMR, UV/Vis, hemolysis assay, flow cytometry, and histological determination of co-prodrug HN−CBL (PDF)

■ AUTHOR INFORMATION

Corresponding Authors

Teng Liu − *Department of Pediatrics, Xiangya Hospital, Central South University, Changsha 410008, PR China*; Phone: +86-731- 89753044; Email: liutengjy@126.com

Yongbo Peng − *Institute of Chinese Medicine, Hunan Academy of Traditional Chinese Medicine&Innovation Centre for Science and Technology, Hunan University of Chinese Medicine, Changsha 410208, PR China; College of Life Science, Molecular Science and Biomedicine Laboratory, State Key Laboratory for Chemo/Bio-Sensing and Chemometrics, Hunan University, Changsha 410082, PR China;* orcid.org/0000-0003-4861-7184; Phone: +86-731-88821894; Email: pengyongbo2000@126.com

Authors

Li Xia − *School of Traditional Chinese Medicine, Guangdong Food and Drug Vocational College, Guangzhou 510520, PR China*

Dali Kang − *School of Traditional Chinese Medicine, Guangdong Food and Drug Vocational College, Guangzhou 510520, PR China; Department of Pediatrics, Xiangya Hospital, Central South University, Changsha 410008, PR China*

Dan Wan − *Institute of Chinese Medicine, Hunan Academy of Traditional Chinese Medicine&Innovation Centre for Science and Technology, Hunan University of Chinese Medicine, Changsha 410208, PR China; College of Life Science, Molecular Science and Biomedicine Laboratory, State Key Laboratory for Chemo/Bio-Sensing and Chemometrics, Hunan University, Changsha 410082, PR China*

Chu Chu − *College of Pharmaceutical Science, Zhejiang University of Technology, Hangzhou 310014, PR China*

Meizi Chen − *Department of General Internal Medicine, The First People's Hospital of Chenzhou, Chenzhou 423000, PR China*

Shuihan Zhang − *Institute of Chinese Medicine, Hunan Academy of Traditional Chinese Medicine&Innovation Centre for Science and Technology, Hunan University of Chinese Medicine, Changsha 410208, PR China*

Xiong Li − *Institute of Chinese Medicine, Hunan Academy of Traditional Chinese Medicine&Innovation Centre for Science and Technology, Hunan University of Chinese Medicine, Changsha 410208, PR China; School of Clinical Pharmacy/The First Hospital, Guangdong Pharmaceutical University, Guangzhou 510006, PR China*

Leye He − *Department of Urological Surgery and Research Institute for Prostate Disease, Third Xiangya Hospital, Central South University, Changsha 410013, PR China*

Jianye Yan − *Institute of Chinese Medicine, Hunan Academy of Traditional Chinese Medicine&Innovation Centre for Science and Technology, Hunan University of Chinese Medicine, Changsha 410208, PR China*

Complete contact information is available at: https://pubs.acs.org/10.1021/acsomega.0c02832

Author Contributions

L.X., D.K., and D.W. contributed equally to this work. The paper was written through contributions of all the authors. All the authors have given approval to the final version of the manuscript.

Notes

The authors declare no competing financial interest.

■ ACKNOWLEDGMENTS

This research was supported by the National Natural Science Foundation of China (81803693), Key Research and Development Project of Hunan Province (2019NK2101), and Natural Science Foundation of Hunan Province (2020JJ5913), the Training Program for Outstanding Young Teachers in Higher Education Institutions of Guangdong Province in 2015 (no. YQ2015196) and Natural Science Fund Project of Guangdong Province (no. 2018A030313225). And we thank for Professor Jun Xu's molecular docking help (School of pharmacy, Jinan University in Guangzhou).

REFERENCES

(1) Langerak, A. W.; Ritgen, M.; Goede, V.; Robrecht, S.; Bahlo, J.; Fischer, K.; Steurer, M.; Trněný, M.; Mulligan, S. P.; Mey, U. J. M.; Trunzer, K.; Fingerle-Rowson, G.; Humphrey, K.; Stilgenbauer, S.; Böttcher, S.; Brüggemann, M.; Hallek, M.; Kneba, M.; van Dongen, J. J. M. Prognostic value of MRD in CLL patients with comorbidities receiving chlorambucil plus obinutuzumab or rituximab. *Blood* **2019**, *133*, 494−497.

(2) Luo, C.-Q.; Zhou, Y.-X.; Zhou, T.-J.; Xing, L.; Cui, P.-F.; Sun, M.; Jin, L.; Lu, N.; Jiang, H.-L. Reactive oxygen species-responsive nanoprodrug with quinone methides-mediated GSH depletion for improved chlorambucil breast cancers therapy. *J. Controlled Release* **2018**, *274*, 56−68.

(3) El Hilali, M.; Reux, B.; Debiton, E.; Leal, F.; Galmier, M. J.; Vivier, M.; Chezal, J. M.; Miot-Noirault, E.; Coudert, P.; Weber, V. Linker structure-activity relationships in fluorodeoxyglucose chlorambucil conjugates for tumor-targeted chemotherapy. *Bioorg. Med. Chem.* **2017**, *25*, 5692−5708.

(4) Millard, M.; Gallagher, J. D.; Olenyuk, B. Z.; Neamati, N. A selective mitochondrial-targeted chlorambucil with remarkable cytotoxicity in breast and pancreatic cancers. *J. Med. Chem.* **2013**, *56*, 9170−9179.

(5) Guan, X.; Chen, Y.; Wu, X.; Li, P.; Liu, Y. Enzyme-responsive sulfatocyclodextrin/prodrug supramolecular assembly for controlled release of anti-cancer drug chlorambucil. *Chem. Commun.* **2019**, *55*, 953−956.

(6) Ma, Z.-Y.; Wang, D.-B.; Song, X.-Q.; Wu, Y.-G.; Chen, Q.; Zhao, C.-L.; Li, J.-Y.; Cheng, S.-H.; Xu, J.-Y. Chlorambucil-conjugated platinum(IV) prodrugs to treat triple-negative breast cancer in vitro and in vivo. *Eur. J. Med. Chem.* **2018**, *157*, 1292−1299.

(7) Singh, R. K.; Kumar, S.; Prasad, D. N.; Bhardwaj, T. R. Therapeutic journery of nitrogen mustard as alkylating anticancer agents: Historic to future perspectives. *Eur. J. Med. Chem.* **2018**, *151*, 401−433.

(8) Rauf, A.; Patel, S.; Imran, M.; Maalik, A.; Arshad, M. U.; Saeed, F.; Mabkhot, Y. N.; Al-Showiman, S. S.; Ahmad, N.; Elsharkawy, E. Honokiol: An anticancer lignan. *Biomed. Pharmacother.* **2018**, *107*, 555−562.

(9) Lin, D.; Yan, Z.; Chen, A.; Ye, J.; Hu, A.; Liu, J.; Peng, J.; Wu, X. Anti-proliferative activity and structure-activity relationship of honokiol derivatives. *Bioorg. Med. Chem.* **2019**, *27*, 3729−3734.

(10) Pan, J.; Lee, Y.; Wang, Y.; You, M. Honokiol targets mitochondria to halt cancer progression and metastasis. *Mol. Nutr. Food Res.* **2016**, *60*, 1383−1395.

(11) Pan, J.; Lee, Y.; Cheng, G.; Zielonka, J.; Zhang, Q.; Bajzikova, M.; Xiong, D.; Tsaih, S.-W.; Hardy, M.; Flister, M.; Olsen, C. M.; Wang, Y.; Vang, O.; Neuzil, J.; Myers, C. R.; Kalyanaraman, B.; You, M. Mitochondria-Targeted Honokiol Confers a Striking Inhibitory Effect on Lung Cancer via Inhibiting Complex I Activity. *iScience* **2018**, *3*, 192−207.

(12) Pan, J.; Lee, Y.; Zhang, Q.; Xiong, D.; Wan, T. C.; Wang, Y.; You, M. Honokiol Decreases Lung Cancer Metastasis through Inhibition of the STAT3 Signaling Pathway. *Cancer Prev. Res.* **2017**, *10*, 133−141.

(13) Liang, X.; Li, X.; Yue, X.; Dai, Z. Conjugation of porphyrin to nanohybrid cerasomes for photodynamic diagnosis and therapy of cancer. *Angew. Chem., Int. Ed. Engl.* **2011**, *50*, 11622−11627.

(14) Chen, X.; Xu, Y.; Li, X.; Liao, S. Fluorogenic approach to evaluating prodrug hydrolysis and stability in live cells. *Bioorg. Med. Chem.* **2019**, *27*, 851−858.

(15) Shen, Y.; Jin, E.; Zhang, B.; Murphy, C. J.; Sui, M.; Zhao, J.; Wang, J.; Tang, J.; Fan, M.; Van Kirk, E.; Murdoch, W. J. Prodrugs forming high drug loading multifunctional nanocapsules for intracellular cancer drug delivery. *J. Am. Chem. Soc.* **2010**, *132*, 4259−4265.

(16) Fonseca, S. B.; Pereira, M. P.; Mourtada, R.; Gronda, M.; Horton, K. L.; Hurren, R.; Minden, M. D.; Schimmer, A. D.; Kelley, S. O. Rerouting chlorambucil to mitochondria combats drug deactivation and resistance in cancer cells. *Chem. Biol.* **2011**, *18*, 445−453.

(17) Santos, J. H.; Hunakova, L. u.; Chen, Y.; Bortner, C.; Van Houten, B. Cell sorting experiments link persistent mitochondrial DNA damage with loss of mitochondrial membrane potential and apoptotic cell death. *J. Biol. Chem.* **2003**, *278*, 1728−1734.

(18) Li, K.; Yang, K.; Zheng, L.; Li, Y.; Wang, Q.; Lin, R.; He, D. Anti-acute myeloid leukemia activity of 2-chloro-3-alkyl-1,4-naphthoquinone derivatives through inducing mtDNA damage and GSH depletion. *Bioorg. Med. Chem.* **2018**, *26*, 4191−4200.

(19) Martinou, J.-C.; Youle, R. J. Mitochondria in apoptosis: Bcl-2 family members and mitochondrial dynamics. *Dev. Cell* **2011**, *21*, 92−101.

(20) Xu, J.; Chen, Y.; Yang, R.; Zhou, T.; Ke, W.; Si, Y.; Yang, S.; Zhang, T.; Liu, X.; Zhang, L.; Xiang, K.; Guo, Y.; Liu, Y. Cucurbitacin B inhibits gastric cancer progression by suppressing STAT3 activity. *Arch. Biochem. Biophys.* **2020**, *684*, 108314.

(21) Peng, Y. B.; Zhao, Z. L.; Liu, T.; Xie, G. J.; Jin, C.; Deng, T. G.; Sun, Y.; Li, X.; Hu, X. X.; Zhang, X. B.; Ye, M.; Tan, W. H. A Multi-Mitochondrial Anticancer Agent that Selectively Kills Cancer Cells and Overcomes Drug Resistance. *ChemMedChem* **2017**, *12*, 250−256.

(22) Liu, Q.; Peng, Y.-B.; Zhou, P.; Qi, L.-W.; Zhang, M.; Gao, N.; Liu, E.-H.; Li, P. 6-Shogaol induces apoptosis in human leukemia cells through a process involving caspase-mediated cleavage of eIF2α. *Mol. Cancer* **2013**, *12*, 135.

https://dx.doi.org/10.1021/acsomega.0c02832
ACS Omega 2020, 5, 19844−19852